Donald G. Leckie*
*Department of Soil Science*
*University of British Columbia*
*Vancouver, B.C. V6T 1W5, Canada*

# An Error Analysis of Thermal Infrared Line-Scan Data for Quantitative Studies

Errors in determining surface temperature, temperature differences between sites, and temperature changes using thermal infrared line-scan data may be large.

## Introduction

Thermal infrared line-scan data have a large potential as a data base for scientific research as well as for applied investigations such as thermal inertia mapping, soil moisture determination, evapotranspiration and sensible heat flux estimation, and vegetation stress detection (e.g., Gillespie and Kahle, 1977; Leckie, 1980a; Cihlar *et al.*, 1979; Heilman *et al.*, 1976; Leckie *et al.*, 1981; Byrne *et al.*, 1979). A prerequisite for such quantitative applications is that accurate surface temperature values may be derived from thermal infrared line-scan data. Digital image processing and display techniques offer a practical method of determining surface temperature. The magnitude and source of errors in determining surface temperatures from digital thermal infrared line-scan data are investigated with respect to the manners in which the data are often used (e.g., temperature, temperature difference between sites, and temperature changes). The purpose of this study is to determine the errors expected for a general remote sensing thermal infrared line-scan survey, utilizing procedures and data commonly available to most users.

Abstract: *The major sources of error in thermal infrared line-scan data are analyzed to determine their effect on temperature measurements as used in quantitative studies. A small error in calibration of detector output to temperature is assumed. Instrument error is analyzed using scanner data from test flights. The effects of atmospheric attenuation and emission are estimated by an additive atmospheric offset equal to the average difference between temperatures of selected sites measured on the ground and measured by the scanner. Error in this offset is evaluated from data of several flights. Error due to emissivity is estimated from theoretical considerations. The probable errors for a typical remote sensing survey using data commonly available to most users were estimated to be, for night and day surveys respectively: 1.2 and 1.7°C for determining surface temperature; 1.6 and 2.3°C for temperature changes of a site between surveys (including errors due to misregistration); and errors from 0.35 to 1.2 and 0.7 to 2.4°C or larger for temperature differences between sites on the same survey. Due to difficulties in estimating surface emissivity and the atmospheric offset, emissivity and atmospheric errors are the most important.*

Errors in surface temperature, as determined by an infrared line scanner, may be considered to have three components:

* Now with Petawawa National Forestry Institute, Canadian Forestry Service, Chalk River, Ontario K0J 1J0, Canada.

© 1982 American Society of Photogrammetry

- system (instrument) and calibration errors,
- atmospheric errors, and
- emissivity errors.

The magnitudes of these three errors are estimated for a simulated scanner system which operates as follows. The scanner sweeps its field of view across the ground surface, and radiation within this field of view and within the bandpass of the scanner causes a response in the detector which is recorded in analog form. It will be assumed that the detector output is linear with the effective radiance causing the signal. This signal is then digitized to pixels with intensity levels between 0 and 255. The scanner system simulated in this study has two internal blackbody reference sources. Their temperatures are known and may be adjusted. One is normally set in the lower range of expected surface temperatures, the other near the higher expected temperatures. During every scan the blackbodies are viewed by the scanner and the signal recorded and subsequently digitized. These data will be used for temperature calibration.

Calibration, system, atmospheric, and emissivity errors are examined in order to determine the expected magnitudes of these errors. The magnitudes of the errors are then used to analyze the total temperature error. Theoretical considerations of the factors governing the response of a detector and the scanner output versus temperature calibration function[1] are discussed. The instrument error is analyzed using data obtained by a Daedalus (Model 1230) thermal infrared line scanner during several flights. The effects of atmospheric attenuation and emission are estimated by comparing thermal line-scan data with temperature measurements on the ground. Errors in this procedure are determined from data of test flights. A theoretical approach is used to investigate emissivity errors, and examples of errors for an 8 to 14 $\mu$m Ge:Hg detector are presented. The total errors are then estimated for typical night and day conditions and described in terms of probable error.[2]

### THEORETICAL CONSIDERATIONS AND CALIBRATION

By the Stephan-Boltzmann law, it is known that the total radiation emitted from a blackbody surface is proportional to the fourth power of surface temperature. The radiation emitted by a surface in the bandpass of a sensor is found by integrating Planck's equation over the bandpass. Planck's equation, giving the spectral distribution of emitted energy in terms of radiance (W/m²/sr), may be expressed as follows:

$$L_\lambda(\lambda, Ts) = 2c^2h\lambda^{-5}(e^{hc/\lambda kTs} - 1)^{-1} \quad (1)$$

where $L_\lambda(\lambda, Ts)$ is the radiance per unit wavelength (spectral radiance), $c$ is the speed of light, $h$ is Planck's constant, $k$ is Boltzmann's constant, $Ts$ is the surface temperature, and $\lambda$ is wavelength.

The response of photon-sensitive detectors to emitted radiation is not a simple relation to temperature, although Dancak (1979) shows that a relation in temperature to the fourth power can give a good approximation. The radiation reaching an airborne detector is, however, also influenced by atmospheric transmittance and emittance as well as the transmission characteristics of the scanner optics. Finally, the spectral response curve of the detector in the bandpass of the system must be considered. The radiance available from a blackbody surface to produce a signal in a detector (effective radiance) may be given as

$$L = \int_{\lambda 1}^{\lambda 2} [L_\lambda(\lambda, Ts)\tau a(\lambda)\tau o(\lambda) + La(\lambda)]R(\lambda)d\lambda \quad (2)$$

where $\lambda_1$ to $\lambda_2$ is the bandpass of the system, $L_\lambda(\lambda, Ts)$ is the spectral radiance of a blackbody given by Equation 1, $R(\lambda)$ is the relative detector response, $\tau a(\lambda)$ is the atmospheric transmission factor, $\tau o(\lambda)$ is the transmission factor for the scanner optics, and $La(\lambda)$ is the spectral radiance due to atmospheric emission and scattered energy that arrive at the detector. Since the response of the detector is assumed linear with the effective radiance, the output signal and, ultimately, the pixel intensity level may be considered proportional to $L$. The precise calibration function, therefore, varies with the type of detector, spectral bandpass, the surface temperature and temperature range over which calibration is desired, and to some extent atmospheric conditions.

Bastuscheck (1970) calculates the energy available to produce a signal in a detector for a given temperature of a blackbody. This available energy is termed "effective energy." He applies Planck's equation, atmospheric transmittance, and detector response over the bandpass of an 8 to 14 $\mu$m mercury-doped germanium (Ge:Hg) detector (Figure 1a). Figure 1b gives the first derivative of the function shown in Figure 1a. Precise calibration functions are not always available, and linear relationships of output pixel intensity level to temperature ($T$ function) and with temperature to the fourth power ($T^4$ function) may often be used. The known signals (pixel intensity levels) and temperatures of the internal blackbody reference sources of the scanner are used to determine the two coefficients of the linear equations relating pixel intensity level to $T$ or to $T^4$. Figure 1a also

---

[1] The calibration function is the equation mapping detector output (pixel intensity levels) to temperature.

[2] Probable error ($R$) is a quantity such that the probability that an error of a measurement will be between $+R$ and $-R$ is one-half and the probability that it will be outside the limits $+R$ and $-R$ is one-half. Error is assumed to be normally distributed. Probable error may be related to mean square error (standard deviation) ($\sigma$) by R = $0.6745\sigma$ and to average error ($\eta$) by R = $0.8453$ $\eta$ (Scarborough, 1962).
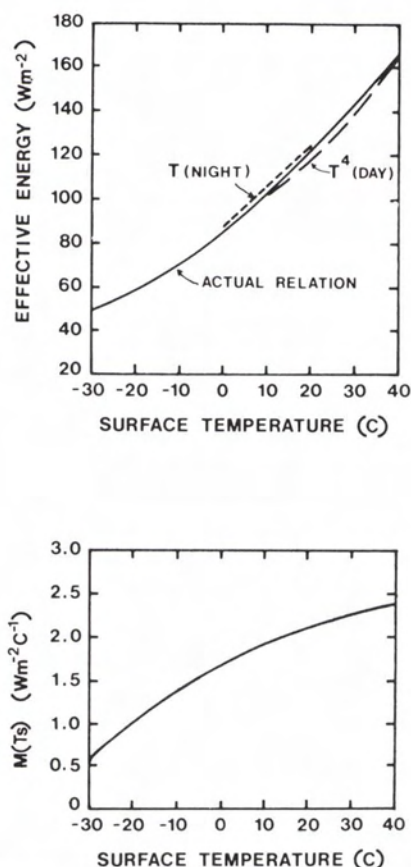
Fig. 1. (a) Effective energy for a Ge:Hg detector as a function of the temperature of a blackbody surface (after Bastuscheck, 1970). Also given are $T^4$ function for a typical day case and $T$ function for a typical night case. (b) Change in effective energy caused by a one degree temperature change ($M(Ts)$) for the Ge:Hg detector (after Bastuscheck, 1970).

shows the $T^4$ function for a typical day case and the $T$ function for a typical night case. The importance of a precise calibration function or a good approximation for a particular sensor is further demonstrated by Scarpace *et al.* (1975).

It will be assumed for the remainder of this study that a good approximation of the precise calibration function is used.

## SYSTEM (INSTRUMENT) ERRORS

Detector, system electronics, and recording noise in the surface-temperature signal, noise in the blackbody reference signals, and inaccurate control of blackbody temperatures are expected to be the main origin of system errors.

The errors in the pixel intensity level of the surface temperature signal (detector, system electronics, and recording noise), also referred to in

this paper as pixel intensity level error, was investigated using thermal line-scan data from a Daedalus (Model 1230) Hg:Cd:Te scanner operating in the 9.5 to 11.5 $\mu$m bandpass. The data were flown and processed by the Canada Centre for Remote Sensing. The blackbody signals were digitized to intensity levels between 0 and 255 for 32 pixels of each blackbody. The magnitude of the pixel intensity level error is estimated by comparing the intensity levels of the same blackbody reference pixel over short periods of time during a flight. A significant change is not expected in blackbody temperature over a short period of time, and corresponding pixel intensity levels of every scan line should be the same.

Table 1 gives the results for several image segments of seven flights. The variation of the intensity levels of the same blackbody pixels, expressed in terms of probable error, is generally between one and seven intensity levels. The temperature resolution of the scanner is given as 0.2°C. Analysis of digitized data (Table 1) indicates that the pixel intensity level error for the daytime flights was not less than for nighttime flights, as might be expected (each intensity level usually represents a larger temperature interval during daytime flights). It is the intent of this paper to describe errors typical of operational surveys; therefore, the subsequent error analysis is in terms of errors in pixel intensity level instead of temperature. This will lead to predicted errors for daytime that are larger than those for nighttime thermal infrared surveys. For example, the temperature interval per pixel intensity level is commonly 0.1 and 0.2°C for night and day surveys, respectively; therefore, errors due to detector, system electronics, and recording noise would range from

TABLE 1. ANALYSIS OF PIXEL INTENSITY LEVEL
ERROR FOR SEVEN FLIGHTS

| Flight (time, date) | Error for blackbody | |
|---|---|---|
| | #1 | #2 |
| 2300, 10/6/77 | 0.9 | 1.3 |
| 2300, 29/7/78 | 6.3 | 1.0 |
| 0400, 11/6/77* | 1.1 | — |
| 0400, 30/7/78 | 5.0 | 6.7 |
| 0900, 11/6/77 | 4.8 | 1.3 |
| 1800, 11/6/77 | 5.5 | 1.5 |
| 1430, 29/7/78 | 4.9 | 6.6 |
| — | Mean = 3.6 | |

Note: Data are taken from six 4-second segments of data 20 seconds apart for each flight. Error is given as the probable error of each of the central 16 blackbody pixels averaged for the 16 blackbody pixels of each data segment and then averaged for the six data segments. Results for six consecutive 0.33-second segments are similar. Scan rate is 60 scans per second. The reason for the contrasting error of blackbody 1 and 2 for some flights is unknown.

* Blackbody #2 was often saturated at pixel intensity level 255.

0.1 to 0.7°C for night surveys and 0.2 to 1.4°C for day surveys, assuming pixel intensity level errors of one to seven intensity levels.

The variation of the pixel intensity levels of the central 16 blackbody pixels of each scan line about their mean is a measure of how accurately the pixel intensity levels of the blackbodies can be determined. The probable error, as might be expected, was found to be similar to the pixel intensity level error.

The other major component of system error is the blackbody temperatures. It is assumed that the probable errors in the temperatures to which the blackbody reference plates can be set and controlled is 0.1°C.[3] It is further assumed that the blackbody temperatures for each scan line are known (with a probable error of 0.1°C) and a correction for changes in blackbody temperature have been applied. Two other factors must also be considered: the blackbody reference plates are not perfect emitters and the temperature may not be uniform across the blackbody plates. Corrections for the imperfect nature of the blackbody plates can be applied if the emissivity of the plates is known. Corrections for temperature nonuniformity can be made if the magnitudes of the temperature variation across the plates are known and are consistent in time. These corrections are assumed to have been applied.

Typical probable errors may be derived from the preceding discussion. Two conditions of error were used in subsequent error analysis: a low error (pixel error #1) had a pixel intensity level probable error and probable error in the mean blackbody pixel intensity level of two intensity levels, and a high error (pixel error #2) had probable errors of seven intensity levels. The probable error in the temperature of the blackbodies was taken to be 0.1°C.

Case 7 of Tables 3 and 4 (Tables to be discussed in further detail in summary of total errors section) gives an analysis of the temperature error resulting from instrument error when a $T$ or $T^4$ calibration function is used (errors are similar for both functions). Typical night and day surveys are considered (Table 5). Noise in surface temperature pixel intensity level is the most important error. Errors in mean blackbody pixel intensity level are also important. Errors for day flights are larger due to the typically wider range of surface temperatures being measured.

## ATMOSPHERIC ERRORS

The effect of the atmosphere between the surface and sensor is both additive and multiplicative

[3] The temperatures of the blackbody reference sources of Daedalus 1200 series line scanners are maintained to within ±0.2°C of their nominal value (i.e., a probable error of 0.13°C) (Daedalus Enterprises Ltd., 1974).

(Equation 2). Since sophisticated techniques for correcting scanner temperatures for atmospheric effects may often require instruments and data not commonly available to many users, a simple correction procedure is investigated. An additive atmospheric correction or offset is applied (i.e., all scanner temperatures are offset or added to by an amount equal to the average difference (offset) between temperature measurements obtained on the ground and scanner temperatures for the same ground truth sites). Offsets obtained from several sites will differ. The magnitude of these differences is a good measure of the errors expected in applying this type of offset. Table 2 gives examples of the expected errors for flights studied by the author and several from the literature. The potential for larger errors is considerable; therefore, typical probable errors likely range between 0.3 and 1.5°C. Two cases will be considered in further error analysis: a high 1.3°C ($\triangle atm_H$), and a low 0.5°C ($\triangle atm_L$) probable error.

The error in the atmospheric offset determined from measurements is largely due to problems in measuring and correlating the temperatures obtained on the ground and by the scanner. These errors may be summarized as follows:

- Extrapolation of ground measurements to the time of the flight (especially during day flights); surface temperature changes with time due to the diurnal temperature wave.
- Short-term local advective effects; instantaneous scanner temperature may not be a characteristic of the micrometeorological conditions at the time of the ground measurements; this effect can be several degrees for vegetated surfaces.

TABLE 2.　ERROR IN DETERMINING ATMOSPHERIC OFFSET

| Flight Number | Probable Error (°C) | Number of Sites |
|:---:|:---:|:---:|
| 1 | 0.9 | 6 |
| 2 | 0.7 | 6 |
| 3 | 1.0 | 7 |
| 4 | 0.3 | 10 |
| 5 | 0.4 | 9 |
| 6 | 0.7 | 4 |
| 7 | 0.9 | 4 |
| 8 | 0.9 | 5 |
| 9 | 0.5 | 5 |
| 10 | 0.9 | 4 |
| 11 | 1.2 | 3 |
| 12 | 0.4 | 32 |
| 13 | 0.4 | 40 |
| — | Mean = 0.7 | — |

Note: The error is expressed as the probable error if the mean of the temperature differences between ground temperature measurements and airborne thermal line-scan temperature measurements of the same sites is taken to be the correct atmospheric offset. Flights 1 to 5 from data of author (ground temperature measured with a calibrated Barnes PRT-10 infrared thermometer), 6 to 11 from data of Heilman et al. (1976), and 12 and 13 from Schott (1979). Flight 12 is 4 flights of 8 sites each flight; flight 13 is 5 flights of 8 sites each flight.

- Errors in ground and scanner measurements.
- Errors in locating ground truth sites on the thermal imagery.

The variation of the atmospheric offset due to differing atmospheric conditions among sites may cause additional errors. The data of flights 1 to 5 of Table 2 were derived for sites of differing vapor pressure (usually $< 100$ Pa) and air temperature ($<2.0°C$) at 1.5 m above the ground surface; therefore, these data have some site variation incorporated into them. There is a systematic change in the atmospheric offset with scan angle due to a lengthening of radiation path length with increasing scan angle. Scarpace et al. (1975) determined, for a flight at 1520 m, that the temperature deviation from a temperature measurement at nadir was 0.1°C at a 30 degree scan angle and up to 0.5°C at a 50 degree scan angle. Temperature deviation from nadir depends on surface temperature, atmospheric conditions, the scanner system, and flying altitude. Schott (1979) also discussed this problem. The atmospheric offset, therefore, depends on the position of the ground truth sites. Because the ground measurements are compared with calibrated thermal infrared data, the atmospheric offset will also depend on the temperature of the ground truth sites with respect to the blackbody temperatures. The atmospheric offset will have an effect of reducing the error in the calibration.

More sophisticated atmospheric correction procedures were discussed by Weiss (1971), Shaw and Irbe (1972), Heilman et al. (1976), Kahle et al. (1979), and Schott (1979). They may aid in reducing error; however, they may often require instrumentation or data not available to many users. Schott's method, which included scan angle correction, reduced the probable error of the corrected temperature data for flights 12 and 13 of Table 2 to 0.17 and 0.18°C, respectively.

## Emissivity Errors

The radiance available to produce a signal in a detector viewing the ground surface (an imperfect radiator) may be given, using Equation 2, by

$$L = \int_{\lambda_1}^{\lambda_2} [\epsilon(\lambda)L_\lambda(\lambda,Ts)\,\tau a\,(\lambda) + L\alpha(\lambda)]R(\lambda)d\lambda \quad (3)$$
$$+ \int_{\lambda_1}^{\lambda_2} [1 - \epsilon(\lambda)]B_\lambda(\lambda)\tau a(\lambda)\tau o(\lambda)R(\lambda)d\lambda$$

where $\epsilon(\lambda)$ is the emissivity of the surface and $B_\lambda(\lambda)$ is the spectral radiance incident at the surface from the atmosphere. The surface is assumed to be Lambertian. Further, assuming emissivity to be constant over $\lambda_1$ to $\lambda_2$, Equation 3 is written as follows:

$$L = \epsilon L_{BB}(Ts) + (1 - \epsilon)B \quad (4)$$

where $L_{BB}$ $(Ts)$ is the effective radiance from a blackbody surface at $Ts$ given by Equation 2 (assuming the difference between $La$ and $\epsilon La$ is

small) and $B$ is the radiance available to produce a signal in the detector due to atmospheric downward radiation if all atmospheric downward radiation were reflected (i.e., second term of Equation 3 evaluated with $\epsilon(\lambda) = 0$).

A calibration function, based on the assumption that the ground surfaces act as blackbodies, will map the output pixel intensity level resulting from an effective radiance ($L$) to a remotely sensed temperature ($Tr$) which does not equal the actual surface temperature ($Ts$). The error due to emissivity may be given by

$$Ts - Tr = [L_{BB}(Ts) - L]/M_L(Ts) \quad (5)$$

where $M_L(Ts)$ is the rate of change of effective radiance with temperature ($\partial L/\partial T$) at $Ts$. Since $\partial L/\partial T$ does not vary greatly over the small temperature errors expected, the above approximation is valid. Substituting Equation 4 into Equation 5 yields

$$Ts - Tr = [1 - \epsilon][L_{BB}(Ts) - B]/M_L(Ts). \quad (6)$$

It may be advantageous to assume a surface emissivity other than one. A correction to transform the calibration function with $\epsilon = 1$ to one with $\epsilon = \epsilon a$($\epsilon a$ is the assumed emissivity used in the calibration) can be derived using Equation 6 with $\epsilon a$ substituted for $\epsilon$. This gives an emissivity error of

$$Ts - Tr_{\epsilon a} = [\epsilon a - \epsilon] [L_{BB}(Ts) - B]/M_L(Ts) \quad (7)$$

where $Tr_{\epsilon a}$ is the temperature given by the new ($\epsilon = \epsilon a$) calibration.

The error is a linear function of the difference between actual and assumed emissivity. The slope is a function of the calibration function of the scanner, surface temperature and $B$. Figure 2 gives the temperature error per 0.01 unit of error in emissivity ($\epsilon - \epsilon a$) for the 8 to 14 $\mu$m Ge:Hg detec-
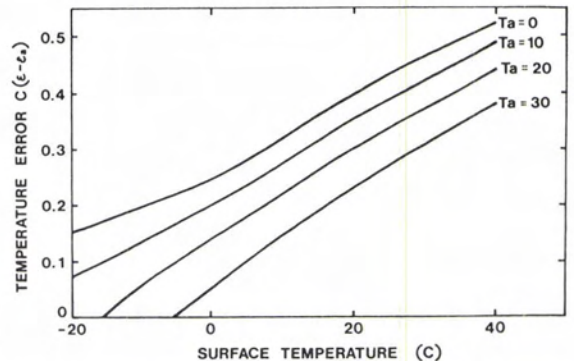


FIG. 2. Temperature error due to assuming an erroneous emissivity. Error is given as the temperature error (°C) for a 0.1 unit error in emissivity estimate ($\epsilon - \epsilon a$) for various atmospheric and surface temperatures. Downward atmospheric radiation is expressed in terms of air temperature at screen height ($Ta$) by an empirical formula of Idso and Jackson (1969).

tor of Figure 1.[4] Lorenz (1966) and Fuchs and Tanner (1966) discussed errors in infrared thermometry caused by emissivity effects.

Neglecting emissivity (i.e., using $\epsilon a=1$) is advantageous because knowledge of $B$ is not required. However, this can lead to large errors. If surface type is known, temperature errors may be reduced by calculating temperature using standard emissivity values for the surface type and measured or estimated $B$. Estimating surface emissivity from values as given in the literature may be difficult, especially if the surface is not uniform. Sutherland and Bartholic (1977) described the example of bare soil patches in terrain with a vegetation cover. If a single estimate of emissivity is used for an entire thermal survey area, errors

[4] $B$ is approximated in this study by determining the fraction of total downward radiation in the bandpass of the scanner using figures of atmospheric downward radiation (Kondratyev, 1969; Idso and Jackson, 1968). This is then applied to the total downward radiation given as a function of air temperature at screen height (Idso and Jackson, 1969). A correction for hemispherical radiation (Lorenz, 1966) is applied. The atmospheric attenuation and detector response are included in a bulk factor for the radiation in the bandpass.

can be large. Three cases will be used in further error analysis: (1) emissivity known; (2) emissivity estimated from standard values (typical probable error in emissivity of about 0.02); and (3) emissivity unknown and/or estimated for a survey area of widely varying emissivity (high probable error in emissivity of 0.05). The latter two cases will also account for most errors caused by assuming a Lambertian surface for many natural surfaces which are actually anisotropic radiators.

## SUMMARY OF TOTAL ERRORS

Tables 3 and 4 indicate the total errors expected in surface temperature determination. The conditions for which errors are estimated represent the range of conditions which are common in thermal infrared surveys. Table 5 indicates the input and conditions for each case. They are derived from the previous discussions. Night and day surveys are considered. Pixel error #1 has low noise levels in the pixel intensity levels of the surface temperature data and the blackbodies, while pixel error #2 has high noise levels. The effect of instrument error is calculated assuming either a calibration function linear with temperature or with temperature to the fourth power; results are similar. For

TABLE 3.   SUMMARY OF ERRORS; DAY CASE

| Case | Contribution to $R^2$ due to probable error | | | | | | | | Totals | | |
| | $p$ | $p_1,p_2$ | $T_1,T_2$ | cal | $atm_L$ | $atm_H$ | $emiss_T$ | $emiss_H$ | $R$ | Max | Rd |
|---|---|---|---|---|---|---|---|---|---|---|---|
| 1 | — | — | — | — | 1.00 | — | — | — | 0.50 | 0.50 | 0.71 |
| 2 | — | — | — | — | — | 1.00 | — | — | 1.3 | 1.3 | 1.8 |
| 3 | — | — | — | — | 0.30 | — | 0.70 | — | 0.92 | 1.3 | 1.3 |
| 4 | — | — | — | — | 0.06 | — | — | 0.94 | 2.0 | 2.4 | 2.8 |
| 5 | — | — | — | — | — | 0.74 | 0.26 | — | 1.5 | 2.1 | 2.1 |
| 6 | — | — | — | — | — | 0.31 | — | 0.69 | 2.3 | 3.2 | 3.3 |
| Pixel Error #1 | | | | | | | | | | | |
| 7 | 0.65 | 0.33 | 0.02 | — | — | — | — | — | 0.50 | 0.90 | 0.70 |
| 8 | 0.65 | 0.32 | 0.02 | 0.01 | — | — | — | — | 0.50 | 0.95 | 0.70 |
| 9 | 0.32 | 0.16 | 0.01 | 0.01 | 0.50 | — | — | — | 0.71 | 1.5 | 1.0 |
| 10 | 0.08 | 0.04 | 0.00 | 0.00 | — | 0.88 | — | — | 1.4 | 2.3 | 2.0 |
| 11 | 0.15 | 0.07 | 0.01 | 0.00 | 0.23 | — | 0.54 | — | 1.0 | 2.2 | 1.4 |
| 12 | 0.04 | 0.02 | 0.00 | 0.00 | 0.06 | — | — | 0.88 | 2.1 | 3.4 | 2.9 |
| 13 | 0.06 | 0.03 | 0.00 | 0.00 | — | 0.67 | 0.24 | — | 1.6 | 3.0 | 2.3 |
| 14 | 0.03 | 0.01 | 0.00 | 0.00 | — | 0.30 | — | 0.66 | 2.4 | 4.2 | 3.4 |
| 15 | 0.19 | 0.10 | 0.01 | 0.00 | — | — | 0.70 | — | 0.92 | 1.7 | 1.3 |
| 16 | 0.04 | 0.02 | 0.00 | 0.00 | — | — | — | 0.94 | 2.0 | 2.2 | 2.8 |
| Pixel Error #2 | | | | | | | | | | | |
| 7 | 0.67 | 0.33 | 0.00 | — | — | — | — | — | 1.7 | 2.9 | 2.4 |
| 8 | 0.67 | 0.33 | 0.00 | 0.00 | — | — | — | — | 1.7 | 3.0 | 2.4 |
| 9 | 0.61 | 0.31 | 0.00 | 0.00 | 0.08 | — | — | — | 1.8 | 3.5 | 2.5 |
| 10 | 0.42 | 0.21 | 0.00 | 0.00 | — | 0.37 | — | — | 2.2 | 4.3 | 3.0 |
| 11 | 0.52 | 0.26 | 0.00 | 0.00 | 0.07 | — | 0.15 | — | 2.0 | 4.2 | 2.8 |
| 12 | 0.28 | 0.14 | 0.00 | 0.00 | 0.04 | — | — | 0.54 | 2.6 | 5.4 | 3.7 |
| 13 | 0.38 | 0.19 | 0.00 | 0.00 | — | 0.32 | 0.11 | — | 2.3 | 5.0 | 3.2 |
| 14 | 0.24 | 0.12 | 0.00 | 0.00 | — | 0.20 | — | 0.44 | 2.9 | 7.5 | 4.1 |
| 15 | 0.55 | 0.28 | 0.00 | 0.00 | — | — | 0.17 | — | 1.9 | 3.7 | 2.7 |
| 16 | 0.29 | 0.15 | 0.00 | 0.00 | — | — | — | 0.56 | 2.6 | 4.9 | 3.7 |

TABLE 4. SUMMARY OF ERRORS; NIGHT CASE

| | Contribution to $R_2$ due to probable error | | | | | | | | Totals | | |
|---|---|---|---|---|---|---|---|---|---|---|---|
| Case | $p$ | $p_1,p_2$ | $T_1,T_2$ | cal | $atm_L$ | $atm_H$ | $emiss_T$ | $emiss_H$ | $R$ | Max | $Rd$ |
| 1 | — | — | — | — | 1.00 | — | — | — | 0.50 | 0.50 | 0.71 |
| 2 | — | — | — | — | — | 1.00 | — | — | 1.3 | 1.3 | 1.8 |
| 3 | — | — | — | — | 0.44 | — | 0.56 | — | 0.75 | 1.1 | 1.0 |
| 4 | — | — | — | — | 0.11 | — | — | 0.89 | 1.5 | 1.9 | 2.1 |
| 5 | — | — | — | — | — | 0.84 | 0.16 | — | 1.4 | 1.9 | 2.0 |
| 6 | — | — | — | — | — | 0.46 | — | 0.54 | 1.9 | 2.7 | 2.7 |
| **Pixel Error #1** | | | | | | | | | | | |
| 7 | 0.62 | 0.31 | 0.07 | — | — | — | — | — | 0.25 | 0.50 | 0.35 |
| 8 | 0.59 | 0.30 | 0.08 | 0.04 | — | — | — | — | 0.26 | 0.55 | 0.37 |
| 9 | 0.12 | 0.06 | 0.02 | 0.01 | 0.79 | — | — | — | 0.54 | 1.1 | 0.80 |
| 10 | 0.02 | 0.01 | 0.00 | 0.00 | — | 0.97 | — | — | 1.3 | 1.9 | 1.9 |
| 11 | 0.06 | 0.03 | 0.01 | 0.00 | 0.40 | — | 0.50 | — | 0.79 | 1.6 | 1.1 |
| 12 | 0.02 | 0.01 | 0.00 | 0.00 | 0.11 | — | — | 0.86 | 1.5 | 2.5 | 2.1 |
| 13 | 0.02 | 0.01 | 0.00 | 0.00 | — | 0.82 | 0.15 | — | 1.4 | 2.4 | 2.0 |
| 14 | 0.01 | 0.01 | 0.00 | 0.00 | — | 0.46 | — | 0.53 | 1.9 | 3.3 | 2.7 |
| 15 | 0.10 | 0.05 | 0.01 | 0.01 | — | — | 0.82 | — | 0.62 | 1.1 | 0.87 |
| 16 | 0.02 | 0.01 | 0.00 | 0.00 | — | — | — | 0.97 | 1.4 | 2.0 | 2.0 |
| **Pixel Error #2** | | | | | | | | | | | |
| 7 | 0.66 | 0.33 | 0.01 | — | — | — | — | — | 0.86 | 1.5 | 1.2 |
| 8 | 0.66 | 0.33 | 0.01 | 0.00 | — | — | — | — | 0.86 | 1.5 | 1.2 |
| 9 | 0.49 | 0.25 | 0.01 | 0.00 | 0.25 | — | — | — | 0.99 | 2.0 | 1.4 |
| 10 | 0.20 | 0.10 | 0.00 | 0.00 | — | 0.70 | — | — | 1.6 | 2.8 | 2.2 |
| 11 | 0.38 | 0.19 | 0.00 | 0.00 | 0.19 | — | 0.24 | — | 1.1 | 2.6 | 1.6 |
| 12 | 0.16 | 0.08 | 0.00 | 0.00 | 0.09 | — | — | 0.67 | 1.7 | 3.4 | 2.4 |
| 13 | 0.18 | 0.09 | 0.00 | 0.00 | — | 0.62 | 0.11 | — | 1.7 | 3.4 | 2.4 |
| 14 | 0.11 | 0.05 | 0.00 | 0.00 | — | 0.39 | — | 0.45 | 2.1 | 4.2 | 3.0 |
| 15 | 0.46 | 0.23 | 0.01 | 0.00 | — | — | 0.30 | — | 1.0 | 2.1 | 1.4 |
| 16 | 0.18 | 0.09 | 0.00 | 0.00 | — | — | — | 0.73 | 1.6 | 2.9 | 2.3 |

each case, examples of low and high atmospheric offset error and typical and high emissivity error are considered. In determining typical probable errors in the calibration function ($\triangle$cal) it was assumed that a good calibration function is used. Also, if an atmospheric offset is applied, this will reduce the error due to calibration. Thirdly, if temperatures of different sites on the same image are compared, the error due to calibration can be quite small, depending on the temperature of each site in comparison to the temperature of the blackbodies and each other. A small probable calibration error (0.05°C) is therefore used.

The contribution to $R^2$ ($R=$ probable error; see Table 5) due to each parameter represents a measure of the importance of error in that parameter to the total error. The probable error in measuring temperature difference between sites or temperature changes of sites is included ($Rd$). Cases 1 to 6 represent examples of errors occurring if it is assumed, as it correctly may be, that the atmospheric offset error accounts also for the system (instrument) and calibration function error of the scanner. The set of all cases represents the combination of errors which may occur under a wide variety of conditions and applications of thermal infrared surveys.

One of the most common uses of thermal infrared surveys is to determine surface temperatures. Errors expected for this application are given by cases 3 to 6 or 11 to 14 of Tables 3 and 4. For site-specific studies in which emissivity and atmospheric offset are known, the error is given by case 8. Cases 9 and 10 give errors for situations in which emissivity is known. Cases 15 and 16 represent the condition of known atmospheric offset but assumed emissivity. Temperature errors for daytime images will range from 0.5 to 2.9°C. For general remote sensing surveys, a typical probable error is likely approximately 1.7°C.[5] Errors for nighttime surveys will generally be smaller, ranging from 0.5 to 2.1°C. A typical probable error for general surveys is approximately 1.2°C.[5] Emis-

[5] Typical probable error for general surveys is derived from intermediate atmospheric offset error (0.9°C; intermediate between $\triangle atm_L$ and $\triangle atm_H$), typical emissivity error, and intermediate pixel error (4.5 intensity levels; intermediate between pixel error #1 and #2).

TABLE 5.  INPUT, CONDITIONS, AND DEFINITIONS FOR TABLES 3 AND 4

| | |
|---|---|
| All cases | $p = 125$ |
| | $\Delta T_1 = \Delta T_2 = 0.1°C$ |
| | $\Delta cal = 0.05°C$ |
| | $\Delta atm_L = 0.5°C, \Delta atm_H = 1.3°C$ |
| | probable error in emissivity is 0.02 |
| | for $\Delta emiss_T$ and 0.05 for $\Delta emiss_H$ |
| Pixel Error #1 | $\Delta p = \Delta p_1 = \Delta p_2 = 2$ intensity levels |
| Pixel Error #2 | $\Delta p = \Delta p_1 = \Delta p_2 = 7$ intensity levels |
| Day all cases | $T_1 = 15°C, T_2 = 55°C$ |
| | $Ts = 35°C$ |
| | $Ta = 25°C$ yields $B = 22$ W m$^{-2}$/sr |
| | $\Delta emiss_T = 0.77°C, \Delta emiss_H = 1.9°C$ |
| | (from Figure 2) |
| Night all cases | $T_1 = 0°C, T_2 = 20°C$ |
| | $Ts = 10°C$ |
| | $Ta = 10°C$ yields $B = 16$ W m$^{-2}$/sr |
| | $\Delta emiss_T = 0.56°C, \Delta emiss_H = 1.4°C$ |
| | (from Figure 2) |

Definitions

$\Delta$ indicates probable error

$p, p_1, p_2,$ = pixel intensity level of surface temperature data, and blackbodies 1 and 2, respectively

$T_1, T_2$ = temperature of blackbodies 1 and 2

$Ta$ = air temperature at screen height

$R$ = probable error, the probable error in $Ts$ where $Ts$ is a function of $q_1, q_2, \ldots, q_n$ as given by

$$R = \left[ \sum_{i=1}^{n} r_i^2 \right]^{1/2}$$

where

$$r_i = \frac{\partial Ts}{\partial q_i} \Delta q_i$$

$$Max = \sum_{i=1}^{n} r_i$$

$Rd$ = probable error for temperature differences ($= \sqrt{2}\, R$)

Contribution to $R^2$ due to $\Delta q_i$ is given by

$$r_i^2/R^2$$

and represents a measure of the contribution of the error in each parameter to $R$.

---

sivity and atmospheric offset errors are the most important.

Temperature differences (relative temperature) between sites on the same image are often required. For sites with the same emissivity, the probable error is given by the $Rd$ of case 7. This is valid only for sites of similar temperature. If the sites differ widely in temperature, the change in emissivity error with temperature (Figure 2) will cause an additional error component. For large temperature differences of approximately 20°C, the additional error component is about 0.15°C per 0.01 unit error in emissivity estimate ($\epsilon - \epsilon a$). Errors in the temperature differences of sites on the same image but with differing emissivities depend on the value of $\epsilon - \epsilon a$ and the temperature of each site. For an example of $\epsilon - \epsilon a < 0.02$ and a difference of $< 0.02$ in the emissivities of the two sites, the magnitude of the errors due to emissivity vary from 0.0 to about 0.8°C for a 20°C temperature difference between sites. Similarly, with $\epsilon - \epsilon a$ in the range 0.00 to 0.05, the emissivities of the sites not differing by more than 0.05, the additional emissivity error will vary in magnitude from 0.0 to 1.9°C. For night images, surface temperature differences are not as large and additional emissivity

errors will be less. Temperature differences between sites of similar temperature and emissivity will be in error by 0.7 to 2.4°C for a day image and 0.35 to 1.2°C for a night image (Tables 3 and 4; case 7). Good accuracies of typical images (temperature and emissivity varying) can be expected to be of the order of 1.0°C for day images and 0.5°C for night images.

Comparison of temperatures of different sites with differing emissivities on separate images can lead to large errors. Errors will depend on $\epsilon - \epsilon a$ and the temperature of each site, as well as the atmospheric conditions during each flight. Since the temperature estimates of the different sites on separate images are independent, typical probable errors in temperature difference may be given by the $Rd$ for cases 3 to 6 or 11 to 14. Errors for comparison of day images will be typically 1.3 to 4.1°C with a typical error of 2.4°C; for night images 1.0 to 3.0°C, typically 1.8°C.[5]

A final important application of thermal infrared line-scan data is the investigation of temperature change of a site in time. The $Rd$ of cases 9 and 10 give estimates of errors in temperature change under conditions of equivalent temperature and atmosphere. These errors are likely good estimates of the error in temperature change between two nighttime surveys taken on the same night. Surface temperature and atmospheric conditions often do not change greatly during a night. Errors will be from 0.8 to 2.2°C, a typical error being about 1.6°C.[6] Comparisons of two day images require an error, in addition to those of cases 9 and 10, due to the variation of emissivity error with surface temperature and atmosphere (Figure 2). An additional error of about 0.05°C per 0.01 unit emissivity error is reasonable.[7] This will yield probable errors from 1.0 to 3.2°C, typical errors being approximately 2.2°C.[8] The additional emissivity error for changes between a day and night image will be high, due to large surface and air temperature differences between day and night. An error of 0.10°C per 0.01 unit emissivity error is reasonable. The range of expected errors is therefore 0.9 to 3.2°C. Typical probable errors for day-night situations are expected to be approximately 2.0°C.[8]

A requirement of temperature change measurement is that the site be accurately located on both images. The effect of misregistration was tested on two image segments from each of four nighttime thermal infrared line-scan surveys and image segments from three day surveys (three image segments for two surveys, two segments for the other). The image segments were 256 by 256 pixels. The terrain was moderate relief natural rangeland of sparse to dense vegetation. All image segments were from one of three test areas. Ground resolution was between 4 and 5 m. There was no smoothing applied to the digital data. Errors in temperature change due to misregistration were assumed to be represented by the temperature differences in pixels a given distance apart on the same image. The average probable error in temperature due to misregistrations of 1.0, 1.4, 2.0, and 2.8 pixels for the above image segments were 0.24, 0.28, 0.33, and 0.40°C, respectively, for the night images and 0.66, 0.84, 1.00, and 1.25°C for the day images. Daytime errors were larger due to the greater variability and range of surface temperatures. Errors will depend on the nature of the surfaces and homogeneity of the surface with respect to the resolution of the processed data.

A good image-to-image registration accuracy for airborne line-scan images is approximately one or slightly more than one pixel in both the along-track and cross-track direction (Leckie, 1980b). A 0.25°C probable error in temperature difference due to misregistration is reasonable for nighttime data. Misregistration will therefore generally have only a small effect on the total probable error except for cases when errors in the other parameters are minimal. Typical probable error for temperature change during the night is therefore approximately 1.6°C. A probable error of 0.8°C represents a case of low error. A reasonable probable error resulting from misregistration of day images is 0.7°C. Total probable errors for temperature changes on two day images are therefore likely to range from 1.2 to 3.3°C, with typical probable errors of 2.3°C. Typical probable errors for day-night temperature changes are expected to be less (approximately 2.1°C).

## CONCLUSIONS

Good estimates of surface emissivity are necessary. Emissivity errors are responsible for a large portion of the error in surface temperature determination. Error in determination of the atmospheric offset was the other major component of error. More sophisticated methods of atmospheric correction should be applied if practicable. System errors, although not as significant as emissivity and atmospheric offset errors, can be important. Calibration function errors are small if a good function is used but choice of a poor calibration function can lead to serious errors. Instrument noise as it affects the surface temperature pixel

---

[6] Typical probable error from intermediate atmospheric offset error (0.9°C) and intermediate pixel error (4.5 intensity levels).

[7] Error corresponds to approximately 10°C change in surface temperature.

[8] Typical probable errors from intermediate atmospheric offset (0.9°C) and intermediate pixel error (4.5 intensity levels) plus additional emissivity error. The additional emissivity error is equivalent to one-half the additional error resulting from an emissivity error ($\epsilon - \epsilon a$) of 0.03.

intensity level is the most important component of system errors.

Errors in determination of surface temperature, temperature differences, and temperature changes can be large. Great care must be taken when using thermal infrared line-scan data in a quantitative manner.

## ACKNOWLEDGMENTS

## REFERENCES

Bastuscheck, C. P., 1970. Ground temperature and thermal infrared. *Photogramm. Eng.* 36(8): 1064–1072.

Byrne, G. F., J. E. Begg, P. M. Fleming, and F. X. Dunin, 1979. Remotely sensed land cover temperature and soil water—a brief review. *Rem. Sens. Env.* 8: 291–305.

Cihlar, J., T. Sommerfeldt, and B. Paterson, 1979. Soil water content estimation in fallow fields from airborne thermal scanner measurements. *Canadian J. Rem. Sens.* 5(1): 18–32.

Dancak, C., 1979. Temperature calibration of fast infrared scanners. *Photogramm. Eng.* 45(6): 749–751.

Daedalus Enterprises Ltd., 1974. *Instruction Manual: Daedalus DS-1200 Series Line Scanner Systems.* Daedalus Enterprises Ltd., Ann Arbor, MI. p. 5-8.

Fuchs, M., and C. B. Tanner, 1966. Infrared thermometry of vegetation. *Agronomy J.* 58: 597–601.

Gillespie, A. R., and A. B. Kahle, 1977. Construction and interpretation of a digital thermal inertia image. *Photogramm. Eng* 43(8): 983–1000.

Heilman, J. L., E. T. Kanemasu, N. J. Rosenberg, and B. L. Blad, 1976. Thermal scanner measurement of canopy temperatures to estimate evapotranspiration. *Rem. Sens. Env.* 5: 137–145.

Idso, S. B., and R. D. Jackson, 1968. Significance of

fluctuation in sky radiant emittance for infrared thermometry. *Agronomy J.* 60: 388–392.

———, 1969. Thermal radiation from the atmosphere. *J. Geophys. Res.* 74(23): 5397–5403.

Kahle, A. B., D. P. Madura, and J. M. Soha, 1979. *Processing of Multispectral Thermal IR Data for Geologic Applications.* JPL Publication 79–89, Jet Propulsion Laboratory, Pasadena, CA. 39 p.

Kondratyev, K. Y., 1969. *Radiation in the Atmosphere.* Academic Press, New York. 912 p.

Leckie, D. G., 1980a. *Development of a nighttime cooling model for remote sensing thermal inertia mapping.* Ph.D. Thesis, Dept. of Soil Science, University of British Columbia, Vancouver, B.C. 246 p.

———, 1980b. Use of polynomial transformations for registration of airborne digital line scan images. *Proceedings Sixth Canadian Symposium on Remote Sensing.* Halifax, Nova Scotia. May 1980. pp. 635–641.

Leckie, D. G., T. A. Black, and P. A. Murtha, 1981. Development and testing of a method of estimating sensible heat flux from natural surfaces using remotely sensed surface temperatures. *Canadian J. Chemical Eng.* 59: 189–194.

Lorenz, D., 1966. The effect of the long-wave reflectivity of natural surfaces on surface temperature measurements using radiometers. *J. Appl. Meteorol.* 5: 421–430.

Scarborough, J. B., 1962. *Numerical Mathematical Analysis.* Oxford University Press, London. 594 p.

Scarpace, F. L., R. P. Madding, and T. Green III., 1975. Scanning thermal plumes. *Photogramm. Eng.* 41(10): 1223–1231.

Schott, J. R., 1979. Temperature measurement of cooling water discharged from power plants. *Photogramm. Eng.* 45(6): 753–761.

Shaw, R. W., and J. G. Irbe, 1972. Environmental adjustments for the airborne radiation thermometer measuring water surface temperature. *Water Resources Res.* 8: 1214–1225.

Sutherland, R. A., and J. F. Bartholic, 1977. Significance of vegetation in interpreting thermal radiation from a terrestrial surface. *J. Appl. Meteorol.* 16(8): 759–763.

Weiss, M., 1971. Airborne measurements of earth surface temperature (ocean and land) in the 10–12 $\mu$m and 8–14 $\mu$m regions. *App. Opt.* 10: 1280–1287.